Pharmaceutical Research, Vol. 22, No. 6, June 2005 (© 2005)
DOI: 10.1007/s11095-005-4593-0

Research Paper

In Vitro/in Vivo Correlation of Transdermal Naltrexone Prodrugs in Hairless Guinea Pigs

Satyanarayana Valiveti,[1,2] Kalpana S. Paudel,[1] Dana C. Hammell,[1] Mohamed O. Hamad,[1] Jianhong Chen,[1] Peter A. Crooks,[1] and Audra L. Stinchcomb[1,3]

Received November 30, 2004; accepted February 25, 2005

Purpose. The purpose of this investigation was to evaluate the *in vitro* and *in vivo* percutaneous absorption of the following prodrugs of naltrexone (NTX): 2′-ethylbutyryl-3-*O*-ester-NTX (ETBUT-ester), methyl-3-*O*-carbonate-NTX (ME-carbonate), ethyl-3-*O*-carbamate-NTX (ET-carbamate), and *N*,*N*-dimethyl-3-*O*-carbamate-NTX (DME-carbamate) in hairless guinea pigs.
Methods. *In vitro* fluxes of NTX and its prodrugs through guinea pig skin were determined using a flow-through diffusion cell system. The pharmacokinetics of NTX prodrugs were determined after topical application of transdermal patches in guinea pigs.
Results. All the prodrugs hydrolyzed to NTX on passing through the skin, and ME-carbonate provided the highest NTX flux and had the highest apparent permeability coefficient (K_p). ME-carbonate and ET-carbamate underwent the highest extent of bioconversion to NTX upon passing through the skin as compared to ETBUT-ester and DME-carbamate. The results of the *in vivo* studies indicated that a significant amount of NTX was delivered after the application of transdermal patches of NTX prodrugs. A mean steady-state plasma concentration of 7.1 ng/ml was obtained after the application of transdermal patches of ME-carbonate. A good correlation was obtained between the *in vitro* and *in vivo* results.
Conclusions. The results of the *in vivo* studies indicated that the ME-carbonate prodrug of NTX was the most promising drug candidate for transdermal delivery.

KEY WORDS: guinea pig; naltrexone; pharmacokinetics; prodrugs; transdermal drug delivery.

INTRODUCTION

The therapeutic efficacy of a drug for transdermal delivery, following its application to skin, mainly depends on its ability to penetrate the skin fast enough to provide the required plasma concentrations that result in the desired pharmacological activity (1). However, for those drugs that do not have the optimal physicochemical properties necessary to achieve therapeutic plasma concentrations via the transdermal route, novel approaches need to be considered in order to increase drug permeation rates through the skin. One of the strategies used to enhance skin permeation is the prodrug approach, which involves the chemical modification of a therapeutic agent such that the delivery rate is improved and conversion to the active drug in the skin and/or body will occur (2). The main advantage of using transdermal prodrugs that can undergo facile biotransformation to the parent drug is that their skin irritation and allergenic potential should only mirror the profile of the active drug, without the possible added toxicities of penetration enhancers or active transport devices. NTX, a potent μ-opioid receptor antagonist (3), is used in the treatment of alcohol dependence and opioid addiction (4,5). NTX undergoes extensive first-pass metabolism upon oral administration with a variable bioavailability ranging from 5–40% (6). NTX was the first new drug approved by the U.S. FDA for the treatment of alcohol dependence in decades, but due to potential patient non-compliance, gastrointestinal adverse effects, and a wide inter-patient variability in metabolism in compliant subjects, the use of NTX for alcoholism treatment has been limited (7–10). Hence, there is a need to develop an alternative non-invasive controlled-release dosage form for this drug. Transdermal delivery of NTX could be an ideal route, due to its advantages of reduction of drug peak-related side effects via zero-order drug delivery, elimination of first-pass metabolism, and the reduction of gastrointestinal side effects seen with oral NTX. Despite the advantages of transdermal delivery, NTX does not have the ideal physicochemical properties (11) necessary to achieve a therapeutic plasma concentration via this route. As a result, a series of prodrugs of NTX, including ester (12), carbonate (13) and carbamate (Vaddi *et al.*; Human skin permeation of 3-O-alkyl carbamate prodrugs of naltrexone. *J. Pharm. Sci.* 2005. Submitted) prodrugs have been synthesized and evaluated for transdermal delivery of NTX using human skin *in vitro* and

[1] Department of Pharmaceutical Sciences, University of Kentucky College of Pharmacy, Lexington, Kentucky, USA.
[2] Present address: Pfizer, Inc., Ann Arbor, Michigan, USA.
[3] To whom correspondence should be addressed. (e-mail: astin2@email.uky.edu)

hairless guinea pigs *in vivo* (14). It was reported that methyl-3-*O*-carbonate-NTX (ME-carbonate) and ethyl-3-*O*-carbamate-NTX (ET-carbamate) provided significant flux increases of NTX across human skin *in vitro*. Also, 2′-ethylbutyryl-3-*O*-ester-NTX (ETBUT-ester) and N,N-dimethyl-3-*O*-carbamate-NTX (DME-carbamate) were thought to be of interest to test *in vivo*, since they, unpredictably, did not improve NTX flux across human skin *in vitro* (15). A good *in vitro*/*in vivo* correlation is always desirable in studies involving transdermal delivery or any other route of drug delivery. In this study, *in vitro* skin permeation studies across hairless guinea pig skin were conducted for the four prodrugs of NTX, and compared with the previous human skin *in vitro* data for these compounds, in order to validate the hairless guinea pig model. *In vivo* studies were carried out in the hairless guinea pig model utlilizing transdermal patches of ETBUT-ester, ME-carbonate, ET-carbamate, and DME-carbamate to establish *in vitro*/*in vivo* correlations.

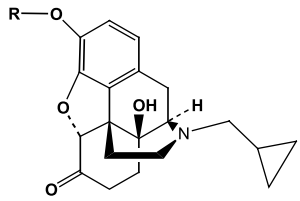

DRUG	R-GROUP	MW	MP(ºC)
NTX	-H	341	174-176
ETBUT-ester	$-COCH(CH_2CH_3)_2$	439	64-67
ME-carbonate	$-COOCH_3$	399	120-121
ET-carbamate	$-CONHCH_2CH_3$	412	78-80
DME-carbamate	$-CON(CH_3)_2$	412	206-208

Fig. 1. Chemical structures, molecular weights, and melting points of NTX and its prodrugs.

MATERIALS AND METHODS

Materials

NTX base was purchased from Mallinckrodt Inc. (St. Louis, MO, USA). All prodrugs were synthesized from NTX free base (Fig. 1). 6-β-Naltrexol (NTXOL) for use as a reference standard was a generous gift from the National Institute on Drug Abuse (Research Triangle Park, NC, USA). Hanks' balanced salts modified powder, sodium bicarbonate, and light mineral oil were purchased from Sigma Chemical (St. Louis, MO, USA). 4-(2-Hydroxyethyl)-1-piperazineethanesulfonic acid (HEPES), gentamicin sulfate, ammonium acetate, ethyl acetate, trifluroacetic acid (TFA), triethylamine (TEA), and acetonitrile (ACN) were obtained from Fisher Scientific (Fairlawn, NJ, USA). 1-octane sulfonic acid sodium salt was obtained from ChromTech (Apple Valley, MN, USA). Ammonium citrate was obtained from Alfa Aesar (Ward Hill, MA, USA). Water was purified by a Barnstead nanopure Diamond Ultrapure water system (Barnstead International, Dubuque, IA, USA). ARcare 7396 (pressure-sensitive tape with MA-38 medical grade acrylic adhesive and 60# Kraft release paper) was a gift from Adhesives Research, Inc. (Glen Rock, PA, USA). MEDIFLEX 1502 (backing membrane; pigmented metalized polyester) was a gift from Mylan Technologies, Inc. (St. Albans, VT, USA). SCOTCHPAK 9742, a fluoropolymer release liner, and CoTran 9715, a 3 mil ethylene vinyl acetate (EVA) copolymer membrane with 19% vinyl acetate, were gifts from 3M Drug Delivery Systems (St. Paul, MN, USA).

Instruments

Equipment used in the current study consisted of a PermeGear flow-through (In-Line, Riegelsville, PA, USA) diffusion cell system, a high pressure liquid chromatograph (HPLC) equipped with a Waters 717plus Autosampler, 1525 Pumps and a 2487 dual wavelength UV absorbance detector with Breeze Chromatography software, and an HPLC with mass spectrometry detection (LC-MS) equipped with a Waters Alliance 2695 pump, Alliance 2690 autosampler, and a Micromass ZQ detector (Milford, MA, USA).

Synthesis of Prodrugs

The prodrugs were synthesized according to the method of Hussain and co-workers (16) with modifications, as previously described (13).

Quantitative Analysis

A modification of the high-pressure liquid chromatography (HPLC) assay described by Hussain *et al.* (16) was used for the analysis of NTX and its prodrugs. The mobile phase comprised of 70:30 ACN: 0.1% TFA with 0.65 g/L 1-octane sulfonic acid sodium salt (adjusted to pH 3.0 with triethylamine). The flow rate of the mobile phase was 1.5 mL/min, and the volume of injection was 100 μL. A Brownlee Valueline C-18 reversed-phase Spheri-5 μm column (220 × 4.6 mm) with a C-18 reversed phase 7 μm guard column (15 × 3.2 mm) was used with the UV/VIS detector set at a wavelength of 215 nm. Standards were analyzed with each set of diffusion samples and exhibited excellent linearity over the entire concentration range employed in the assays. The sensitivity of the assay was 10 ng/ml and 50 ng/ml for NTX and the prodrugs, respectively.

The drugs were extracted from the buffer samples by solid phase extraction (30 mg 1 cc Oasis HLB, Waters Corp., Milford, MA, USA). Before loading the aqueous diffusion samples (5 mL), the cartridge was conditioned with 1 mL of methanol and 1 mL of water. After loading the sample, the cartridge was washed with 1 mL of 5% methanol in water and the drug was eluted with acetonitrile. Sample recoveries were >85% for NTX and the prodrugs.

In Vitro Studies

In Vitro Permeability Studies Across Hairless Guinea Pig Skin

Hairless guinea pigs were sacrificed by pentobarbital overdose. The full thickness skin was removed by blunt dissection and was dermatomed to a thickness of approximately 200 μm. The samples were either used immediately or frozen at −20°C. All animal studies were approved by the University of Kentucky IACUC and the research adhered to the Principles of Laboratory Animal Care. The skin surface temperature of the diffusion cells was maintained at 32°C with a circulating water bath. The diffusion cells were sterilized with 70% v/v ethanol before mounting the guinea pig skin samples into the cell. The receiver solution was HEPES-buffered Hanks' balanced salts with gentamicin at a pH of 7.4 and a flow rate of 1.1 ml/h. These diffusion study conditions were chosen in order to optimize tissue viability according to previous studies by Collier *et al.* (17). A saturated NTX or prodrug solution in light mineral oil was applied to the skin, and each cell was charged with 0.25 mL of the respective drug solution. Samples were collected in six hour increments for 48 h. All the samples were stored at 4°C, until processed by solid phase extraction.

Drug disposition in the skin samples was measured at the end of the 48 h experiment. The skin tissue was rinsed with filtered water and blotted with a paper towel. To remove the drug formulation adhering to the surface, the skin was tape stripped twice using Scotch™ tape. The area of skin in contact with the drug was cut out, minced with a scalpel, and placed in a pre-weighed vial. Drug was extracted from the skin by equilibrating with ten milliliters of acetonitrile at 32°C while shaking (60 rpm) in a water bath overnight. Samples were analyzed by HPLC to determine NTX and prodrug content in micromole of drug per gram of wet tissue weight.

In Vitro Permeability Studies Across EVA Copolymer Membrane-PSA

The permeability of NTX or prodrugs across the CoTran 9715 laminated with PSA was also investigated in order to determine the influence of the rate controlling membrane. The experimental conditions were the same as mentioned above except EVA membrane-PSA (CoTran 9715 laminated with PSA) was mounted in place of the skin.

In Vitro Data Analysis

The cumulative quantity of NTX equivalents collected in the receiver compartment was plotted as a function of time. The flux value for a given experiment was obtained from the slope (steady-state portion) of the cumulative amount of drug permeated vs. time plot. Apparent permeability coefficient values were computed from Fick's First Law of diffusion:

$$\frac{1}{A}\left(\frac{dM}{dt}\right) = J_s = K_p C \qquad (1)$$

In Eq. (1), J_s is the steady-state flux, M is the cumulative amount of drug permeating the skin, A is the area of the skin (0.95 cm^2), K_p is the effective permeability coefficient in cm/h, and ΔC is the difference in concentrations of NTX or prodrug in the donor and receiver solutions. Sink conditions were maintained in the receiver throughout the experiment, so ΔC was approximated by the drug concentration in the donor compartment.

In Vivo Studies in Guinea Pigs

Fabrication of Transdermal Patches

The drug reservoir formulations of prodrugs (14 mg/mL of NTX base equivalent) were prepared in mineral oil, vortexed and sonicated for 5 min. All solutions were saturated and contained excess solid. The transdermal patches of prodrugs of NTX (7.25 cm^2 diffusional area) were fabricated by sandwiching the drug reservoir between a drug-impermeable backing laminate (MEDIFLEX 1502) and an EVA membrane (CoTran 9715) with ARcare 7396 adhesive. A release slip composed of SCOTCHPAK 9742 was used to leave a small opening into the reservoir of the empty device. The membrane/adhesive laminate was heat-sealed to the metalized polyester backing membrane. The slip was removed to form a small port, and the drug solution (500 μL) was injected into the reservoir. After injecting the drug solution into the reservoir, the port was heat-sealed. The TTS patch was kept in a sealed aluminum pouch to minimize the loss of solvent.

Animal Studies

Male and female Hairless IAF and Hartley guinea pigs (Charles River) weighing 335–491 g were used for intravenous studies (n = 5 to 6 per treatment group). For topical studies, male hairless guinea pigs were used (n = 5 to 6). Prior to surgery, the animals were treated with glycopyrrolate and buprenorphine (to induce analgesia), and then ketamine (100 mg/kg, IP) and xylazine (8 mg/kg, IM) were used to induce anesthesia. Catheters were surgically implanted into the jugular vein. A baseline "blank" plasma sample was drawn from each animal immediately before drug treatment. For topical delivery studies, the developed TTS patches (two patches, 14.5 cm^2 diffusional area) were applied to the dorsal region of the hairless guinea pigs. The blood samples were obtained for 48 h while the patches were on the animal, and for another 48 h after patches were removed. Blood samples were drawn for 48 h following the intravenous doses. All animal studies were approved by the University of Kentucky IACUC. The blood samples were immediately centrifuged at 10,000 × g for 3 min; plasma was separated and stored at −70°C until analysis by LC-MS. No significant differences were observed between data from male and female animals after intravenous administration, so the mean values from the combined data of both sexes were used for calculating the predicted steady state concentrations from the *in vitro* flux.

Plasma Sample Extraction Procedure

Exactly 1 mL of acetonitrile:ethyl acetate (1:1, v/v) was added to 0.1 mL of plasma sample in a 1.5-mL microcentrifuge

tube, and the mixture was vortexed for 30 s and centrifuged at 10,000 × g for 20 min. The supernatant was decanted into a clean test tube and evaporated under nitrogen at 37°C. The residue was reconstituted with 100 μL of acetonitrile, vortexed, and sonicated for 5 min. The clear solution was placed into a clean HPLC vial containing low volume inserts, and 20 μL of the sample was injected into the LC-MS system. The extraction efficiency was 93 ± 4% for NTX, 92 ± 5% for NTXOL, 89 ± 6% for ETBUT-ester, 90 ± 8% for ME-carbonate, 93 ± 6% for ET-carbamate, and 92 ± 5% for DME-carbamate. NTXOL is a major active metabolite of NTX.

LC-MS Conditions

LC-MS Conditions for NTX, ME-Carbonate, ET-Carbamate, and DME-Carbamate

Chromatography was performed on a Waters Symmetry C_{18} (2.1 × 150 mm, 5 μm) column at 35°C with a mobile phase consisting of ammonium acetate (2 mM) containing 0.01 mM ammonium citrate:acetonitrile (35:65 v/v) at a flow-rate of 0.25 mL/min. A Waters Symmetry C_{18} (2.1 × 10 mm, 3.5 μm) guard column was used. The volume of injection was 20 μL. The MS detection was performed using electrospray ionization (ESI) for ion production. Selected ion monitoring (SIM) was performed in the positive mode for NTX, *m*/*z* 324 (dwell time 0.30 s), NTXOL, *m*/*z* 344, ME-carbonate, *m*/*z* 400 (dwell time 0.30 s), ET-carbamate, *m*/*z* 413 (dwell time 0.30 s), and DME-carbamate, *m*/*z* 413 (dwell time 0.30 s). The capillary voltage was 4.5 kV and the cone voltage was 50 V. The source block and desolvation temperatures were 120°C and 250°C, respectively. Nitrogen was used as a nebulization and drying gas at flow rates of 50 and 450 L/h, respectively. The retention times for NTX, NTXOL, ME-carbonate, ET-carbamate, and DME-carbamate were 4.90 ± 0.20 min, 3.45 ± 0.23 min., 8.85 ± 0.16 min, 9.51 ± 0.15 min., and 8.20 ± 0.15 min., respectively.

LC-MS Conditions for ETBUT-Ester

The mobile phase composition was: (A) ACN and (B) 2 mM ammonium acetate containing 0.01 mM ammonium citrate and 5% ACN. The mobile phase gradient conditions were as follows: 35% A for 8.0 min followed by a linear gradient to 80% A in 0.5 min, then 80% A for 18 min, and a linear gradient to 35% A in 0.50 min. Between each run the column was equilibrated for 5 min at 35% A. The flow rate was 0.25 mL/min and the temperature of the column was maintained at 35°C. The volume of injection was 20 μL. MS was performed using electrospray ionization (ESI) for ion production. Selected ion monitoring (SIM) was performed in the positive mode for NTX, *m*/*z* 324 (dwell time 0.30 s), NTXOL, *m*/*z* 344 (dwell time 0.30 s), and ETBUT-ester, *m*/*z* 440 (dwell time 0.30 s). The capillary voltage was 4.5 kV and the cone voltage was 50 V. The source block and desolvation temperatures were 120°C and 250°C, respectively. Nitrogen was used as a nebulization and drying gas at flow rates of 50 and 450 L/h, respectively. The retention times for NTX, NTXOL, and ETBUT-ester were 5.65 ± 0.15 min, 4.15 ± 0.13 min, and 17.20 ± 0.25, respectively.

Pharmacokinetic Analysis

Topical administration data were analyzed by non-compartmental analysis to determine peak concentration (C_{max}), lag time to steady-state concentration (t_{lag}) and area under the curve from 0 to 48 h, AUC_{0-48}. The steady state plasma concentration of NTX after the application of patches containing prodrugs was calculated by using the equation:

$$C_{ss} = AUC_{0-t}/time \quad (2)$$

Data Analysis

Statistical analysis of the *in vitro* permeability parameters and pharmacokinetic parameters was computed with a one-way ANOVA followed by Tukey's *post hoc* analysis using SIGMASTAT (SPSS Inc., Chicago, IL, USA).

RESULTS AND DISCUSSION

In Vitro Guinea Pig Skin Diffusion and Concurrent Biotransformation of the NTX Prodrugs

The flux of the prodrug was obtained from the slope of the linear portion of cumulative amount of NTX generated from the prodrug, and the prodrug itself, in NTX equivalents permeated *vs.* time curve. Figure 2 shows a representative profile used to calculate the steady state flux of the ME-carbonate prodrug and NTX released from the ME-carbonate prodrug. All prodrugs hydrolyzed on passing through the skin, and appeared as a combination of NTX and intact prodrug in the receiver solution. Each prodrug was tested in two different hairless guinea pig donor skin samples, using NTX as a control for each set. The flux of NTX from each prodrug and NTX control flux from each group of individual experiments is shown in Fig. 3. As shown in Table I, the flux of NTX from the ME-carbonate prodrug was higher than that for all the other prodrugs, and ME-carbonate was the only prodrug in the present study which provided a higher flux than NTX free base ($p < 0.01$). ETBUT-ester and ET-

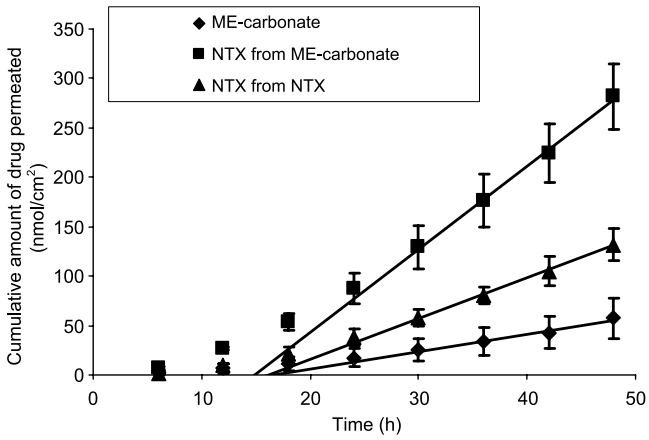

Fig. 2. Representative permeation profile for the diffusion of NTX, NTX from ME-carbonate, and ME-carbonate from saturated solutions through hairless guinea pig skin at 32°C. Data represents mean (±SD) (n = 3 to 4 cells for prodrug and NTX from the skin of two individual animals).

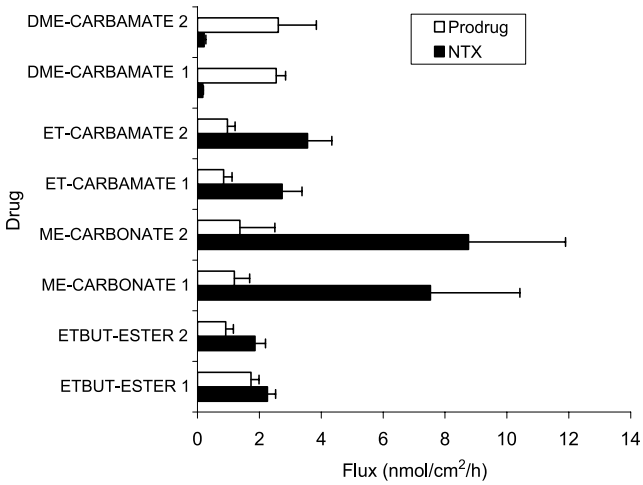

Fig. 3. *In vitro* NTX flux and prodrug flux in guinea pig skin. Data is represented as mean (±SD) (n = 3 to 4 cells).

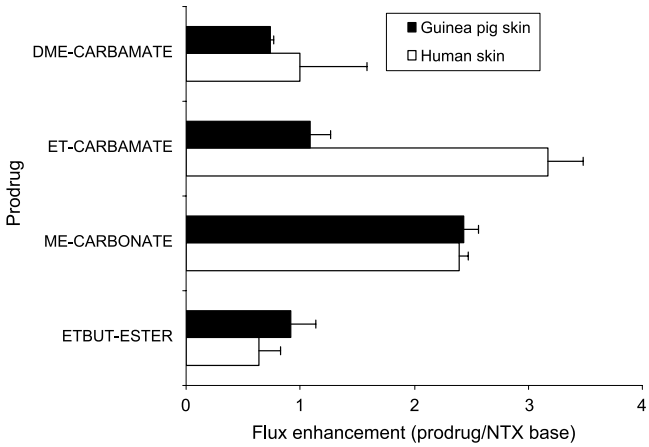

Fig. 4. Comparative profiles of ratio of the total drug flux (NTX + prodrug) from prodrugs to NTX flux from NTX base in guinea pig skin and human skin. [Human skin data reproduced from Vaddi *et al.*; Human skin permeation of 3-O-alkyl carbamate prodrugs of naltrexone. *J. Pharm. Sci.* 2005. Submitted, Vaddi *et al*. (15) and Pillai *et al*. (13).]

carbamate exhibited similar permeation to NTX, where as DME-carbamate exhibited lower permeation than NTX (Table I). The flux enhancement was calculated from each diffusion study as the ratio of prodrug NTX equivalent flux to NTX flux (Fig. 4). The fluxes of NTX from the two prodrugs, ETBUT-ester and DME-carbamate, were not higher than that from the corresponding prodrugs, HEX-ester (12) and ET-carbamate. In fact, the HEX-ester flux was significantly higher than the branched-chain ETBUT-ester flux, and the former straight-chain prodrug was considered to be a promising NTX prodrug (12). The partition coefficients between stratum corneum and mineral oil, and the relative thermodynamic activities of branched chain prodrugs were previously reported to be lower than those of straight chain prodrugs (13,15). Melting points alone were not as predictive in this comparison as relative thermodynamic activities calculated from heats of fusion, in addition to melting points. Calculated log octanol water partition coefficients were also not as useful as measured stratum corneum-vehicle partition coefficients in predicting permeation. The branched chain prodrug (ETBUT-ester and DME-carbamate) were also more enzymatically stable, and did not hydrolyze in plasma and skin as readily when compared with the prodrugs, HEX-ester (12) and ET-carbamate (13,15). During skin permeation, it is expected that ester, carbamate, and carbonate prodrugs will be converted to parent drug by esterase enzymes (18). Skin disposition studies at the end of a 48 h diffusion experiment measuring both NTX and prodrugs showed that all prodrugs in this study were bioconverted 7–80% to NTX during permeation (Fig. 5). ME-carbonate and ET-carbamate generated a higher percentage of NTX than ETBUT-ester and DME-carbamate prodrugs. The bioconversion of the prodrugs in skin can influence the flux of the drugs (19,20). It is possible that a prodrug that undergoes bioconversion in the skin can lead to an increase in flux by a factor of $\sqrt{kD}$, where k is the bioconversion rate constant and D is the diffusivity of the drug in the viable tissue (21). Therefore, larger bioconversion rate constants can increase the flux of the prodrug by creating a higher concentration gradient for the prodrug across the skin (19). Because ETBUT-ester and DME-carbamate prodrugs bioconverted to the parent drug to a lesser extent, it appears that their slower bioconversion rates may have contributed to their slower permeation across the skin than the ME-carbonate and ET-carbamate prodrugs. Valiveti *et al.* (14) reported that the permeation of straight chain ester prodrugs of NTX

Table I. Properties of NTX and Its Prodrugs

Drug	Light mineral oil solubility (mM)	Hanks' buffer solubility (mM)	*NTX flux from mineral oil (nmol/cm^2/h)		*Mean permeability coefficient ($K_p \times 10^4$), cm/h	
			Human skin	Guinea pig skin	Human skin	Guinea pig skin
NTX	0.24 ± 0.02[b]	5.6 ± 0.40[b]	2.9 ± 0.74[b]	3.7 ± 0.92	121[b]	155
ETBUT-ester	5.60 ± 0.25[a]	0.27 ± 0.02[a]	1.97 ± 0.56[a]	3.4 ± 0.84	3.5[a]	6.1
ME-carbonate	0.33 ± 0.02[b]	3.0 ± 0.06[b]	6.9 ± 0.50[b]	9.1 ± 0.47	209[b]	185
ET-carbamate	1.01 ± 0.09[c]	14.2 ± 0.25[c]	15.5 ± 11.3[c]	4.1 ± 0.66	153[c]	40
DME-carbamate	0.20 ± 0.00[c]	3.0 ± 0.05[c]	2.9 ± 0.87[c]	2.8 ± 0.10	147[c]	138

*n = 3 for NTX and n = 4 for prodrugs in human skin. n = 4 for NTX and prodrugs in guinea pig skin.
[a] Values obtained from Vaddi *et al.* (15) and the corresponding NTX flux from NTX was 3.06 nmol cm^{-2} h^{-1}.
[b] Values obtained from Pillai *et al*. (13).
[c] Values obtained from Vaddi *et al.*; Human skin permeation of 3-O-alkyl carbamate prodrugs of naltrexone. *J. Pharm. Sci.* 2005. Submitted and the corresponding NTX flux from NTX was 3.68 nmol cm^{-2} h^{-1}.

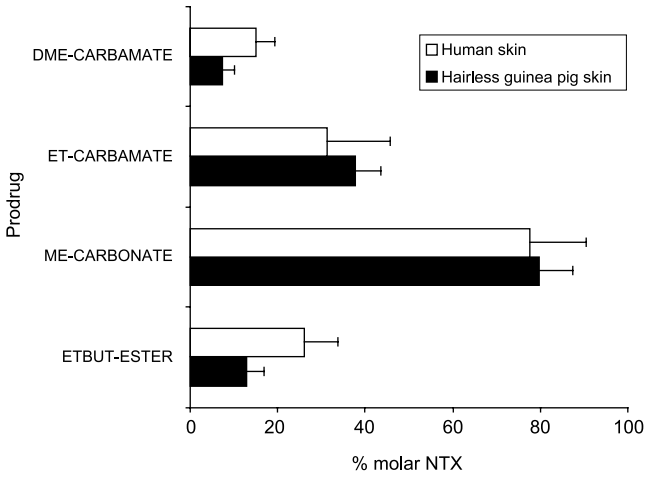

Fig. 5. Drug disposition in hairless guinea pig skin (n = 4) and human skin (n = 4) after 48 h permeation experiment following application of saturated drug solutions in mineral oil. Data represents the mean (±SD) molar percentage of regenerated NTX to total drug extracted from the skin. [Human skin data reproduced from Vaddi *et al.*; Human skin permeation of 3-O-alkyl carbamate prodrugs of naltrexone. *J. Pharm. Sci.* 2005. Submitted, Vaddi *et al.* (15) and Pillai *et al.* (13).]

in guinea pig skin (predicted from *in vivo* data) were not significantly different to 1.8 times higher than in human skin, depending on the prodrug. In the current study, this same relationship was observed (Table I), except for ET-carbamate, which afforded an increase in NTX permeation in human skin (Vaddi *et al.*; Human skin permeation of 3-O-alkyl carbamate prodrugs of naltrexone. *J. Pharm. Sci.* 2005. Submitted). As can be seen in Fig. 5, there were no significant differences in the drug dispositions of the prodrugs in guinea pig skin when compared with the reported data in human skin (13, Vaddi *et al.*; Human skin permeation of 3-O-alkyl carbamate prodrugs of naltrexone. *J. Pharm. Sci.* 2005. Submitted, 15). Based on the current results, hairless guinea pig is an appropriate *in vivo* model for the evaluation of promising NTX transdermal prodrugs, except perhaps in the case of the ET-carbamate.

In Vitro Permeability Studies Across EVA Copolymer Membrane-PSA

In the current study, reservoir type transdermal patches were fabricated in order to provide a reservoir for drug formulation and maintain intimate contact with the skin for at least 48 h, so that *in vitro*/*in vivo* correlations could be evaluated. Additionally, the *in vitro* permeability of NTX and its prodrugs across the EVA copolymer membrane-PSA were carried out in order to provide valuable information about the drug delivery rate control. Hence, *in vitro* studies across EVA copolymer membrane-PSA were completed. Literature reports have shown that EVA membrane (CoTran 9715, 19% w/w of vinyl acetate content) (14,22) laminated with PSA provides very high drug flux rates, as compared to other membrane choices. Hence, in the present study CoTran 9715 laminated with PSA was chosen as a membrane for the fabrication of the patches, where the drug solution was sandwiched between this membrane and the backing membrane. Figure 6 shows *in vitro* diffusion profiles of NTX equivalents from NTX (14), ETBUT-ester, ME-carbonate, ET-carbamate, and DME-carbamate across CoTran 9715 laminated with PSA. The *in vitro* permeation studies indicated that the flux of NTX from NTX, ETBUT-ester, ME-carbonate, ET-carbamate, and DME-carbamate was about 2.3 to 9.6 times (Table II) higher than that through guinea pig skin. The cumulative amount (nmol/cm^2) of NTX permeated across the EVA membrane/PSA/guinea pig skin was 221 nmol/cm^2, 191 nmol/cm^2, 390 nmol/cm^2, 171 nmol/cm^2, and 149 nmol/cm^2, respectively for NTX, ETBUT-ester, ME-carbonate, ET-carbamate, and DME-carbamate, and were predicted from the *in vivo* steady state plasma con-centration (Table III). Guy and Hadgraft (23) proposed that comparison of the amount of drug released in a given period (48 h) from the delivery system alone (M_{device}) with the corresponding amount when the device was placed in contact with skin (M_{total}) would reveal the respective contributions of the device and the skin to the overall rate control.

$$F_D = M_{\text{total}}/M_{\text{device}} \tag{3}$$

Where F_D is the fractional rate control by the device. If the values for the fractional rate control by the device are less than unity, it implies that the delivery rate is controlled by the skin and the device. When the cumulative amount of NTX permeated (nmol/cm^2) from EVA membrane/PSA laminate and the predicted (predicted from the *in vivo* data) cumulative amount (Table II) of NTX permeated (nmol/cm^2) from guinea pig skin/EVA membrane/PSA laminate in 48 h (Table II) were substituted into the above equation, and the values for the fractional rate control by the device were less than unity (0.15 to 0.49) (Table II). These results indicated that the fractional rate control was mainly controlled by the skin, 51–85%. This is important in a study where *in vitro*/*in vivo* correlation was the main goal.

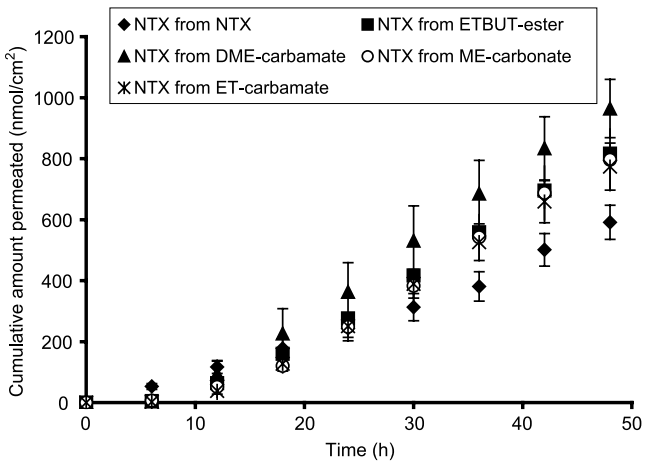

Fig. 6. Profile of mean (±SD) cumulative amount of NTX permeated from NTX,* ETBUT-ester, ME-carbonate, ET-carbamate, and DME-carbamate across EVA copolymer membrane (CoTran 9715)-PSA (n = 4). [*Profile reproduced from Valiveti *et al.* (14).]

Table II. *In Vitro* Data for NTX and Its Prodrugs Across EVA/PSA Membrane and Hairless Guinea Pig Skin

Parameter	NTX	ETBUT-ester	ME-carbonate	ET-carbamate	DME-carbamate
In vitro flux (nmol cm^{-2} h^{-1}) from EVA membrane/PSA	12.2 ± 1.8	27.6 ± 3.8	22.2 ± 3.5	22.6 ± 1.7	26.4 ± 3.0
In vitro flux (nmol cm^{-2} h^{-1}) from EVA membrane/PSA/guinea pig skin[a]	4.6 ± 0.3	3.97 ± 0.97	8.1 ± 1.8	3.6 ± 0.8	3.1 ± 0.3
Cumulative amount permeated (nmol cm^{-2} 48 h^{-1}) across EVA membrane/PSA	512 ± 56	817 ± 14	796 ± 101	774 ± 77	964 ± 96
Cumulative amount permeated (nmol cm^{-2} 48 h^{-1}) from EVA membrane/PSA/guinea pig skin[a]	221 ± 14	191 ± 47	390 ± 84	171 ± 41	149 ± 12
F_D[b]	0.43	0.23	0.49	0.22	0.15

Data represent mean ± SD, $n = 4$.
[a] Values predicted from guinea pig *in vivo* data.
[b] F_D = fractional rate control by the device = M_{total}/M_{device} (values <1 indicates skin is contributing to the control process).

Pharmacokinetic Studies of NTX and Its Prodrugs in Hairless Guinea Pigs

In the current study, LC-MS was used to quantitate the amounts of NTX, NTXOL, and the prodrugs of NTX (ETBUT-ester, ME-carbonate, ET-carbonate, and DME-carbamate) in guinea pig plasma. The utility of these assays was remarkable because of the ability to quantitate prodrug, drug, and metabolite in one small volume of plasma. NTXOL levels were important to measure because NTX undergoes extensive hepatic metabolism, primarily via reduction, to this major active metabolite in humans (24). NTXOL is believed to be a major contributor to the pharmacologic effect of NTX in humans, so it is important to identify and quantitate this compound in a preclinical animal model that may eventually be used for pharmacokinetic/pharmacodynamic correlation. In the current study, we used a slight modification of the LC-MS method of Valiveti *et al.* (14). The NTX, NTXOL, ETBUT-ester, ME-carbonate, ET-carbamate, and DME-carbamate peaks were well resolved and free of interference from endogenous compounds in the plasma. No significant matrix effect was observed for the analytes in the plasma samples. The lower limit of quantitation (LLOQ) was 1.25 ng/ml for NTX and NTXOL, and 0.5 ng/ml for ETBUT-ester, ME-carbonate, ET-carbamate, and DME-carbamate. The postpreparative stability studies indicated that the stabilities of NTX, NTXOL, ETBUT-ester, ME-carbonate, ET-carbamate, and DME-carbamate were greater than 95% for at least 48 h at 12°C (the autosampler temperature).

The plasma concentration profiles of NTX following the application of ETBUT-ester, ME-carbonate, ET-carbamate, and DME-carbamate transdermal patches in hairless guinea pigs are shown in Fig. 7. The pharmacokinetic parameters, including C_{max}, T_{max}, C_{ss}, AUC_{0-48}, and T_{lag} (time to reach steady-state plasma concentration) are given in Table III. The mean steady state NTX plasma concentrations of 4.2 ng/ml, 3.5 ng/ml, 7.1 ng/ml, 3.1 ng/ml, and 2.7 ng/ml were maintained over 48 h for NTX (14), ETBUT-ester, ME-carbonate, ET-carbamate, and DME-carbamate, respectively. The NTX steady state plasma concentration (7.1 ng/ml) from ME-carbonate was significantly higher ($p < 0.001$) than that from NTX base (4.2 ng/ml) and other prodrugs. However, the steady-state plasma concentrations of NTX from ETBUT-ester, ET-carbamate, and DME-carbamate were not significantly ($p > 0.05$) higher than that of NTX itself. It can be seen from Fig. 7 that a significant skin reservoir effect was not observed, as plasma levels of NTX declined after the removal of the patches, at a rate similar to the drug elim-ination rate. A significant amount of intact prodrug was observed in some of the plasma samples, which was con-verted into NTX equivalents and incorporated into the total NTX plasma concentration from the prodrug. However, only trace amounts of NTXOL were observed in some of the plasma samples, and these amounts were not enough to make a significant difference to the total drug plasma concentrations. The results of the present study indicated that ME-carbonate was the most promising NTX prodrug candidate for transdermal delivery.

Table III. Pharmacokinetic Parameters of NTX from NTX Base, ETBUT-Ester, ME-Carbonate, ET-Carbamate, and DME-Carbamate After the Application of the Transdermal Patches in Hairless Guinea Pigs

Parameter	NTX[a]	ETBUT-ester	ME-carbonate	ET-carbamate	DME-carbamate
AUC_{0-48} (ng h/ml)	201 ± 16	167 ± 41	341 ± 74	149 ± 35	130 ± 10
C_{max} (ng/ml)	5.4 ± 0.5	2.7 ± 0.5	8.8 ± 2.0	3.8 ± 0.9	3.0 ± 0.3
T_{max} (h)	20.2 ± 9.7	10.4 ± 7.9	19.7 ± 15.0	16.7 ± 13.3	12.5 ± 8.2
Observed C_{ss} (ng/ml)	4.2 ± 0.3	3.5 ± 0.8	7.1 ± 1.5	3.1 ± 0.7	2.7 ± 0.2
Predicted C_{ss} (ng/ml)	3.3 ± 0.8	3.0 ± 0.7	7.9 ± 0.4	3.4 ± 0.6	2.4 ± 0.1
T_{lag} (h)	4.7 ± 3.7	11.8 ± 10.6	11.4 ± 10.1	9.5 ± 9.2	2.5 ± 1.3
Enhancement factor	1	0.8 ± 0.2	1.7 ± 0.4	0.8 ± 0.2	0.6 ± 0.1

Data represent mean ± SD, $n = 5$ to 6.
[a] Data reproduced from Valiveti *et al.* (14).

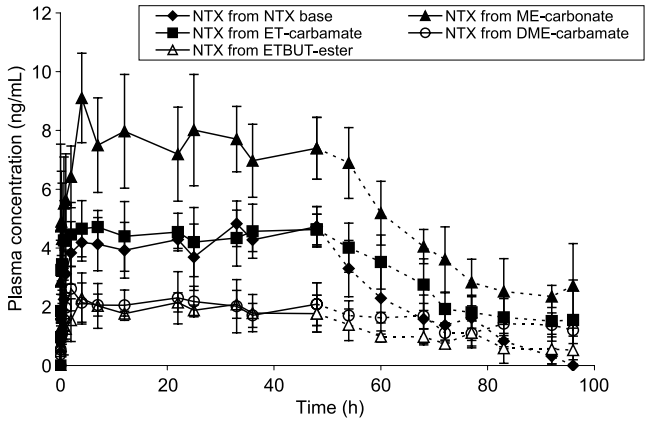

Fig. 7. Mean (±SD) plasma profiles of NTX in guinea pigs (n = 5 to 6) after the application of transdermal patches containing NTX,* ETBUT-ester, ME-carbonate, ET-carbamate, or DME-carbamate. The dotted line (---) indicates the plasma concentration after the removal of patches. [*NTX profile reproduced from Valiveti *et al.* (14).]

In Vitro and *in Vivo* Correlation

Pharmacokinetic parameters such as total body clearance (CL) from intravenous administration of NTX in guinea pigs were required in order to calculate the *in vivo* transdermal flux of NTX from the topical treatment plasma concentration data. In a previous study (14), the pharmacokinetics were investigated after intravenous administration (3 mg/kg) in guinea pigs. The predicted steady state plasma concentration of NTX in the guinea pig following the application of the TTS patches containing NTX, ETBUT-ester, ME-carbonate, ET-carbamate, and DME-carbamate was calculated from *in vitro* guinea pig skin permeability data (Table I), and is shown in Table III. This was calculated by using the following equation:

$$C_{ss} = J_{ss}A/CL \quad (4)$$

where C_{ss} is the predicted steady state plasma concentration (ng/ml); J_{ss} is the steady-state flux from *in vitro* guinea pig skin (Table II); A is area of the applied patch (14.5 cm^2); CL is the total body clearance (5650 mL/h). In the current study, the mean steady state plasma concentrations of NTX following the application of the TTS patches in guinea pigs were 4.2 ng/ml, 3.5 ng/ml, 7.1 ng/ml, 3.1 ng/ml, and 2.7 ng/ml, respectively, for NTX, ETBUT-ester, ME-carbonate, ET-carbamate, and DME-carbonate. There were no significant differences ($p > 0.05$) between the observed and predicted steady state plasma concentrations, except for NTX ($p < 0.04$) (Table III), which had a slightly higher plasma concentration than the predicted plasma concentration. This may be due to differences in enzymatic activity *in vivo vs. in vitro*, or possibly due to a significant contribution to the more polar NTX diffusion via shunt routes in the skin *in vivo*. Nonetheless, these results were quite close, and indicated good *in vitro*/*in vivo* correlation overall. This suggests that the hairless guinea pig is an appropriate *in vivo* model for the evaluation of promising NTX transdermal prodrugs.

The observed *in vivo* lag times were either similar or shorter than lag times observed *in vitro*. Often flow-through diffusion cells artificially add extra time to *in vitro* lag times, because of the way the samples are collected at a relatively slow flow rate. Typically *in vitro* data has exhibited longer lag times for NTX than for the prodrugs, which doesn't seem to hold true *in vivo* where all of the plasma concentration profiles appear to have a similar lag time to steady state. It is possible that NTX lag times are reduced *in vivo* if there is a significant contribution from the shunt routes for the more polar NTX.

CONCLUSIONS

In the current investigation, *in vitro* and *in vivo* evaluation of NTX transdermal prodrugs incorporating three different chemical linkages was completed in hairless guinea pigs, for the purpose of identifying the most promising prodrugs for eventual human use. *In vitro* permeation studies of ETBUT-ester, ME-carbonate, ET-carbamate, and DME-carbamate were conducted across hairless guinea pig skin and EVA copolymer membrane-PSA. *In vivo* pharmacokinetic studies were conducted by the application of transdermal patches containing ETBUT-ester, ME-carbonate, ET-carbamate, and DME-carbamate in hairless guinea pigs. The *in vitro* guinea pig skin studies indicated that ME-carbonate provided the highest NTX flux when compared with NTX and the other prodrugs. The flux enhancements and drug dispositions of the prodrugs in guinea pig skin were not significantly different when compared with the reported data from human skin, except in the case of ET-carbamate. The results of the *in vivo* studies indicated that the 48-h mean steady-state NTX plasma concentrations from ETBUT-ester, ME-carbonate, ET-carbamate, and DME-carbamate were 3.5 ng/ml, 7.1 ng/ml, 3.1 ng/ml, and 2.7 ng/ml, respectively. The observed steady state plasma levels were in good agreement with the predicted steady state plasma levels from the *in vitro* data. The results of the *in vivo* studies indicated that the ME-carbonate prodrug of NTX was the most promising drug candidate for transdermal delivery.

ACKNOWLEDGMENTS

This project was funded by NIH grant R01DA13425. The authors would also like to thank NIDA for supplying the NTXOL, Mylan Technologies, Inc. (St. Albans, VT, USA) for supplying MEDIFLEX 1502, 3M Drug Delivery Systems (St. Paul, MN, USA) for supplying the SCOTCHPAK 9742 and CoTran 9715, and Adhesives Research, Inc. (Glen Rock, PA, USA) for providing ARcare 7396.x

REFERENCES

1. F. P. Bonia, C. Puglia, T. Barbuzzi, P. de Caprariis, F. Palagiano, M. G. Rimoli, and A. Saija. *In vitro* and *in vivo* evaluation of polyoxyethylene esters as dermal prodrugs of ketoprofen, naproxen and diclofenac. *Eur. J. Pharm. Sci.* **14**:123–134 (2001).
2. A. Vigroux, M. Bergon, and C. Zedde. Cyclization-activated prodrugs: N-(substitued 2-hydroxyphenyl and 2-hydroxypropyl) carbamates based on ring-opened derivatives of active benzox-

azolones and oxazolidinones as mutual prodrugs of acetaminophen. *J. Med. Chem.* **38**:3983–3994 (1995).
3. A. E. Takemori and P. S. Portoghese. Selective naltrexone-derived opioid receptor antagonists. *Annu. Rev. Pharmacol. Toxicol.* **32**:239–269 (1992).
4. J. R. Volpicelli, A. I. Alterman, and M. Hayashida. Naltrexone in the treatment of alcohol dependence. *Arch. Gen. Psychiatry* **49**:876–880 (1992).
5. L. Terenius. Rational treatment of addiction. *Curr. Opin. Chem. Biol.* **2**:541–547 (1998).
6. PDR Generics. Medical Economics, 2nd ed., New Jersey, 1996, pp. 2229–2233.
7. J. R. Volpicelli, K. C. Rhines, J. S. Rhines, L. A. Volpicelli, A. I. Alterman, and C. P. O'Brien. Naltrexone and alcohol dependence. Role of subject compliance. *Arch. Gen. Psychiatry* **54**: 737–742 (1997).
8. K. Verebey. The clinical pharmacology of naltrexone: pharmacology and pharmacodynamics. *NIDA Res. Monogr.* **28**:147–158 (1980).
9. R. S. Croop, E. B. Faukner, and D. F. Labriola. The safety profile of naltrexone in the treatment of alcoholism. Results from the multicentre usage study. The naltrexone usage group study. *Arch. Gen. Psychiatry* **54**:1130–1135 (1997).
10. A. C. King, J. R. Volpicelli, M. Gunduz, C. P. O'Brien, and M. J. Kreek. Naltrexone biotransformation and incidence of subjective side effects: a preliminary study. *Alcohol. Clin. Exp. Res.* **21**:906–909 (1997).
11. A. Naik, Y. N. Kalia, and R. H. Guy. Transdermal drug delivery: overcoming the skin's barrier function. *Pharm. Sci. Technol. Today* **3**:318–326 (2000).
12. A. L. Stinchcomb, P. W. Swaan, O. Ekabo, K. E. Harris, J. Browe, D. C. Hammell, T. A. Cooperman, and M. Pearsall. Straight-chain naltrexone ester prodrugs: diffusion and concurrent biotransformation in human skin. *J. Pharm. Sci.* **91**:2571–2578 (2002).
13. O. Pillai, M. O. Hamad, P. A. Crooks, and A. L. Stinchcomb. Physicochemical evaluation, *in vitro* human skin diffusion, and concurrent biotransformation of 3-O-alkyl carbonate prodrugs of naltrexone. *Pharm. Res.* **21**:1146–1152 (2004).
14. S. Valiveti, D. C. Hammell, K. S. Paudel, M. O. Hamad, P. A. Crooks, and A. L. Stinchcomb. *In vivo* evaluation of 3-O-alkyl ester transdermal prodrugs of naltrexone in hairless guinea pigs. *J. Control. Release* **102**:509–520 (2005).
15 H. K. Vaddi, M. O. Hamad, J. Chen, S. L. Banks, P. A. Crooks, and A. L. Stinchcomb. Human skin permeation for branched chain 3-O-alkyl ester and carbonate prodrugs of naltrexone. *Pharm. Res.* **22**(5):758–765 (2005).
16. M. A. Hussain, C. A. Koval, M. J. Myers, E. G. Shami, and E. Shefter. Improvement of the oral bioavailability of naltrexone in dogs: a prodrug approach. *J. Pharm. Sci.* **76**:356–358 (1987).
17. S. W. Collier, N. M. Sheikh, A. Sakr, J. L. Lichtin, R. F. Stewart, and R. L. Bronaugh. Maintenance of skin viability during *in vitro* percutaneous absorption/metabolism studies. *Toxicol. Appl. Pharmacol.* **99**:522–533 (1989).
18. P. G. Hewitt, J. Perkins, and S. A. M. Hotchkiss. Metabolism of fluroxypyr, fluroxypyr methyl ester, and the herbicide fluroxypyr methylheptyl ester. I: during percutaneous absorption through fresh rat and human skin *in vitro*. *Drug Metab. Dispos.* **28**: 748–754 (2000).
19. D. C. Hammell, M. Hamad, H. K. Vaddi, P. A. Crooks, and A. L. Stinchcomb. A duplex "Gemini" prodrug of naltrexone for transdermal delivery. *J. Control. Release* **97**:283–290 (2004).
20. H. Bando, S. Mohri, F. Yamashita, Y. Takakura, and M. Hashida. Effects of skin metabolism on percutaneous penetration of lipophilic drugs. *J. Pharm. Sci.* **86**:759–761 (1997).
21. C. D. Yu, J. L. Fox, N. F. H. Ho, and W. I. Higuchi. Physical model evaluation of topical prodrug delivery-simultaneous transport and bioconversion of vidarabine-5′-valerate I: physical model development and II: parameter determinations. *J. Pharm. Sci.* **68**:1341–1357 (1979).
22. S. Valiveti, D. C. Hammell, D. C. Earles, and A. L. Stinchcomb. Transdermal delivery of the synthetic cannabinoid WIN 55, 212-2: *in vitro*/*in vivo* correlation. *Pharm. Res.* **21**:1137–1145 (2004).
23. R. H. Guy and J. Hadgraft. Rate control in transdermal delivery? *Int. J. Pharm.* **82**:R1–R6 (1992).
24. K. Verebey, J. Volavka, S. J. Mule, and R. B. Resnick. Naltrexone: disposition, metabolism, and effects after acute and chronic dosing. *Clin. Pharmacol. Ther.* **20**:315–328 (1976).